Incorporating habitat distribution in wildlife disease models: conservation implications for the threat of squirrelpox on the Isle of Arran

M. F. Macpherson[1,2,3], R. S. Davidson[2], D. B. Duncan[1], P. W. Lurz[4], A. Jarrott[5] & A. White[1]

1 Department of Mathematics and the Maxwell Institute for Mathematical Sciences, Heriot-Watt University, Edinburgh, UK
2 Disease Systems, SRUC, Edinburgh, UK
3 Computing Science and Mathematics, School of Natural Sciences, University of Stirling, Stirling, UK
4 Royal (Dick) School of Veterinary Studies, The University of Edinburgh, Midlothian, UK
5 Galloway Forest District, Forestry Commission Scotland, Newton Stewart, UK

Abstract

Emerging infectious diseases are a substantial threat to native populations. The spread of disease through naive native populations will depend on both demographic and disease parameters, as well as on habitat suitability and connectivity. Using the potential spread of squirrelpox virus (SQPV) on the Isle of Arran as a case study, we develop mathematical models to examine the impact of an emerging disease on a population in a complex landscape of different habitat types. Furthermore, by considering a range of disease parameters, we infer more generally how complex landscapes interact with disease characteristics to determine the spread and persistence of disease. Specific findings indicate that a SQPV outbreak on Arran is likely to be short lived and localized to the point of introduction allowing recovery of red squirrels to pre-infection densities; this has important consequences for the conservation of red squirrels. More generally, we find that the extent of disease spread is dependent on the rare passage of infection through poor quality corridors connecting good quality habitats. Acute, highly transmissible infectious diseases are predicted to spread rapidly causing high mortality. Nonetheless, the disease typically fades out following local epidemics and is not supported in the long term. A chronic infectious disease is predicted to spread more slowly but can remain endemic in the population. This allows the disease to spread more extensively in the long term as it increases the chance of spread between poorly connected populations. Our results highlight how a detailed understanding of landscape connectivity is crucial when considering conservation strategies to protect native species from disease threats.

Introduction

The heterogeneous distribution and connectivity of habitat has a complex relationship with population abundance and persistence (Bienen, 2002). When habitat is sparse, isolated habitat patches can be formed dividing a population into several subpopulations (Hanski & Gilpin, 1991). Poor connectivity between patches may result in a reduction of movement between local populations which in turn can act to decrease patch biodiversity (Kareiva & Wennergren, 1995), fitness due to inbreeding (Chesser & Ryman, 1986) and population growth (Travis, 2003). Furthermore, poor connectivity may lead to a higher probability of local extinction (Fahrig & Merriam, 1985; Henein & Merriam, 1990; Schumaker, 1996) and reduced likelihood of natural re-establishment via dispersal (Fahrig & Merriam, 1985; van

Andel & Aronson, 2012). Evidence therefore supports the maintenance of dispersal corridors to promote growth and local population persistence and diversity (Beier & Noss, 1998; Dobson *et al.*, 1999; Lookingbill *et al.*, 2010; van Andel & Aronson, 2012). However, enhanced connectivity between subpopulations can increase the spread of infectious disease leading to detrimental impacts on native populations (Hess, 1994; Real & Biek, 2007).

Emerging infectious diseases (EIDs) contribute to species extinction (Smith, Sax & Lafferty, 2006) and are a global threat to biodiversity (Morse, 1995; Daszak, 2000; Daszak, Cunningham & Hyatt, 2001). Morse (1995) proposed that EIDs were caused by a two-step process: the deliberate or accidental introduction of non-native species and/or disease into a susceptible population, and their subsequent establishment within the new environment. The exposure of sus-
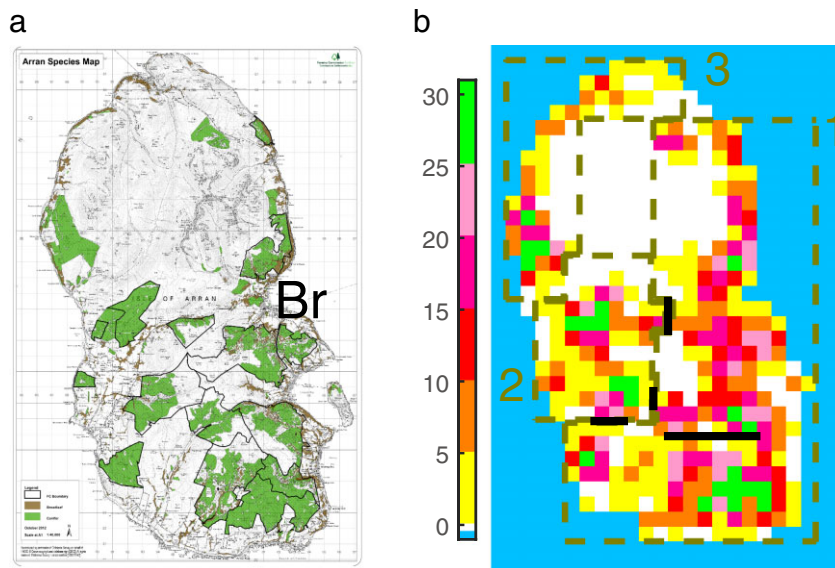
Figure 1 The Isle of Arran is shown in (a) (with permission from Forestry Commission Scotland) with the coniferous (green) and broadleaf (brown) woodland highlighted and 'Br' represents the main port Brodick. The carrying capacity of red squirrels (per km²) is shown in (b) which uses upper density estimates of abundance of 0.36 ha⁻¹ in coniferous and 0.6 ha⁻¹ in broadleaf. Cells that are well connected are grouped together by the dashed olive blocks (labelled regions 1–3); there is poor connectivity between the blocks. In addition, ground-truthing in collaboration with Forestry Commission Scotland has identified routes that do not permit movement, identified by thick black lines.

ceptible indigenous populations to novel and potentially fatal disease may cause population declines and in turn impact species competition, habitat and decrease biodiversity (Manchester & Bullock, 2000). One of the many examples of emergent infectious diseases (Daszak, 2000) is the fungal pathogen *Chalara fraxinea*, believed to have emerged in Poland in 1992 and has since caused widespread die back in Ash species (up to 90% mortality) across Europe (Worrell, 2012). Understanding the spread of EIDs may be crucial to the conservation of native species. Therefore, understanding how disease spreads in the environment can help reduce the impact of infectious disease in wildlife and humans (Patz *et al.*, 2004).

The use of spatial frameworks in mathematical models to explore the impact of infectious disease in wildlife has been well established (Hanski & Gilpin, 1991; Hess, 1996; Hanski, 1998; Keeling, 1999; Rushton *et al.*, 2000; Real & Biek, 2007). Previous theoretical studies that have examined infection dynamics have used classical Levins (1969) meta-population approaches (Hess, 1996; McCallum & Dobson, 2002); simulation methods with an idealized spatial set-up, such as patches connected in a linear or looped array (Hess, 1996; White *et al.*, 2014); or a two-dimensional lattice of homogeneous patches (Cross *et al.*, 2005). However, despite the heterogeneity of natural landscapes and habitats, the incorporation of detailed, realistic landscape structure has been less well explored (Ostfeld, Glass & Keesing, 2005). A realistic representation of landscape structure may consist of a fragmented mixture of high- and low-quality subpopulations with different levels of interpopulation connectivity. Moreover, for directly transmitted parasites, susceptible individuals must encounter an infected individual for infection to spread (Riley, 2007); thus, the inclusion of geographical data in spatial disease models may identify corridors aiding the spread of infectious disease which in turn may be used to contain outbreaks (Beier & Noss, 1998; Dobson *et al.*, 1999; Riley, 2007). We therefore extend the

work of previous studies by considering a heterogeneous spatial set-up derived from real habitat information. A key question will be to understand how results translate between idealized and realistic landscapes.

To illustrate the importance of modelling disease spread in complex environments, we examine the impact of habitat distribution and connectivity on the spread of infectious disease in the Eurasian red squirrel *Sciurus vulgaris* on the Isle of Arran (Fig. 1a). The Eurasian red squirrel has been in decline in mainland United Kingdom since the introduction of the North American grey squirrels *Sciurus carolinensis* in the late 19th century. Initially, competition alone was blamed for causing the reduction in the native population. However, it is now accepted that disease-mediated invasion is a critical factor in the replacement of red squirrels (Daszak, 2000; Rushton *et al.*, 2000; Tompkins, White & Boots, 2003). The emerging squirrelpox virus (SQPV) is likely to have been introduced to the United Kingdom with the grey squirrels (as it is largely avirulent in greys) (Bosch & Lurz, 2012). Squirrelpox causes high mortality in red squirrels and is critical in explaining the rapid replacement of reds (Tompkins *et al.*, 2003). To prevent species extinction, the UK Biodiversity Action Plan (Joint Nature Conservation Committee, 2012) has designated 35 red squirrel strongholds (18 in Scotland and 17 in England), and it is therefore important to understand the threat of SQPV in these strongholds. One such stronghold, Arran, was chosen for its island status and lack of grey squirrels thus far (Lurz, 2012). Arran is roughly 32 by 20 km in dimensions with 6803 ha of fragmented woodland, predominately coniferous, with a mixture of high and low connectivity between local patches (Fig. 1) (Lurz, 2012). Constructing a spatial disease framework based on red squirrels on Arran provides an ideal case study to examine the impact habitat connectivity has on the spread of infectious disease.

Our aims are therefore twofold. First, our case study provides species- and location-specific results that can

directly inform conservation management and policy decisions. Second, we aim to provide a general assessment of the importance of replicating geographical information accurately in spatial models when analysing disease spread in complex landscapes. Therefore, in addition to considering the spread of SQPV, we modify the model to include a range of disease parameters – chronic and acute disease with high and low transmissibility – and so can infer how the complexity of the landscape interacts with disease characteristics to determine the spread and persistence of disease. Moreover, we include two levels of connectivity: one derived directly from geographical information software (GIS) data and one that is additionally supplemented with ground-truthing from local experts that indicate additional barriers to dispersal. We therefore provide a general understanding of how landscape connectivity and infectious disease properties influences disease spread and persistence.

Methods

Red squirrel carrying capacity

We extrapolated woodland data from the forest inventory maps for 2011 [provided by the Forestry Commission Scotland (FCS) website] using GRASS GIS (Westervelt *et al.*, 1992; using similar methods to Rushton *et al.*, 2000 and Lurz, Geddes & Lloyd, 2003). The island was divided into a 1×1 km grid, because 1 km is typically the maximum dispersal distance for red squirrels (Bosch & Lurz, 2012) and larger than the typical 150-m radius of core range activity (which is based on estimates of red squirrels home range of 9 ha; Tonkin, 1983; Lurz, 1995; Bosch & Lurz, 2012). Within each grid cell habitat data identifying no coverage (thus unable to support red squirrels), coniferous and broadleaf woodland was determined from inventory records (shown in Fig. 1a). Published densities of red squirrel abundance in different tree species from Lurz (2012) were used to calculate the carrying capacity for each cell dependent on the quantity and type of woodland cover (Fig. 1b). We used upper density estimates for abundance (which represents repeated high seed years and therefore a worst case scenario for disease spread) with results for lower density estimates (repeated poor seed years) shown in the Supplementary Information.

The model

We assume that any grey squirrels/disease introduced to Arran would be the result of an accidental or deliberate release at the main port (Brodick) on the island (Fig. 1a). Contingency plans have been developed on Arran to trap and remove greys should they be sighted, but this may not prevent disease transmission to the established local red squirrel population and so our initial conditions assume a local population of reds is infected. We base our approach on that of Tompkins *et al.* (2003), who modelled squirrelpox

in both red and grey squirrels on mainland United Kingdom. Here we use the equivalent model for a population of red squirrels only, giving

$$\frac{dS}{dt} = (a - qH)H - bS - \beta SI \quad (1a)$$

$$\frac{dI}{dt} = \beta SI - (b + \sigma)I \quad (1b)$$

for susceptible (S) and infected (I) individuals, in which the total population $H = S + I$. Reds are born susceptible with maximum reproduction rate a and natural mortality rate b. We assume the carrying capacity K is positive and relates to the crowding coefficient $q = (a - b)/K$ that acts to limit the birth rate when the density is high relative to the carrying capacity. Infection is directly transmitted with transmission coefficient β and infected red squirrels experience additional mortality (virulence) at rate σ due to the disease. There is no recovery class as SQPV is lethal to red squirrels (Tompkins *et al.*, 2002).

Initially, there are a small number of infected red squirrels so it is important to include the possibility of disease extinction or fade outs. Therefore, we develop a stochastic version of the deterministic model in equation (1) as this captures the random variability of infectious disease at low densities. Furthermore, in heterogeneous spatial environments the spread of infection may be dictated by rare dispersal events and spatial, probabilistic frameworks can highlight these key dispersal routes. Therefore, within each 1 by 1 km landscape cell (Fig. 1b), we represent the dynamics using a spatial, stochastic model. The rates of change in the deterministic model are turned into probabilities of events (Table 1, see Renshaw, 1993 and Keeling & Rohani, 2008 for details on the methodology) that account for changes in abundance within each grid patch. In addition, the abundance within patches can change due to dispersal and disease spread between neighbouring cells.

We assume squirrels core movement has a range α km (approximated as a circle with diameter of 0.3 km in this study; Bosch & Lurz, 2012) that may include crossing cell boundaries. Therefore, infection can occur through susceptible infected contact within a focal cell (i, j) at rate $\beta S_{i,j} I_{i,j}$ and additionally through contact with neighbouring cells at a rate

$$\beta S_{i,j}\left(\frac{\alpha}{2}\Sigma I_a + \frac{\alpha^2}{4}\Sigma I_c\right) \quad (2)$$

where the ΣI_a represents the contributions from the neighbouring adjacent cells and the ΣI_c the corner cells, see Section S3 of the Supplementary Information for more details. Core range activity is significantly less than the grid cell dimensions and individuals are likely to return to their focal cell and so we ignore these daily dispersal events. However, we include long-distance dispersals where an individual leaves the focal cell (i, j) and enters a neighbouring cell ($i*, j*$). We assume saturation dispersal such that individuals are more likely to disperse as cell density increase

Table 1 A list of all possible events in the model described in The Model section

Description	Outcome	Probability
Birth	$\Pr(S_{i,j} \rightarrow S_{i,j} + 1)$	$[(a - q_{i,j}H_{i,j})H_{i,j}]/R$
Natural death of S	$\Pr(S_{i,j} \rightarrow S_{i,j} - 1)$	$[bS_{i,j}]/R$
Natural death of I	$\Pr(I_{i,j} \rightarrow I_{i,j} - 1)$	$[bI_{i,j}]/R$
Disease-induced mortality	$\Pr(I_{i,j} \rightarrow I_{i,j} - 1)$	$[\sigma I_{i,j}]/R$
Dispersal of S	$\Pr(S_{i,j} \rightarrow S_{i,j} - 1, S_{i^*,j^*} \rightarrow S_{i^*,j^*} + 1)$	$[D_{i,j}S_{i,j}]/R$
Dispersal of I	$\Pr(I_{i,j} \rightarrow I_{i,j} - 1, I_{i^*,j^*} \rightarrow I_{i^*,j^*} + 1)$	$[D_{i,j}I_{i,j}]/R$
Transmission of disease	$\Pr(S_{i,j} \rightarrow S_{i,j} - 1, I_{i,j} \rightarrow I_{i,j} + 1)$	$\left[\beta S_{i,j} \left(\dfrac{\alpha^2}{4} \Sigma I_c + \dfrac{\alpha}{2} \Sigma I_a + I_{i,j} \right) \right] \Big/ R$

The outcome of each event in cell (i, j) is given in column 2 with the associated probability in column 3, where the rate (within square brackets) is divided by the total sum of the rates $R = \Sigma$ [*rates*] across all the cells. The dispersal of susceptible and infected individuals from the focal cell (i, j) to a neighbouring cell (i, j) is given by $D_{i,j}$ which is defined in equation (3). The transmission of disease occurs when a susceptible individual comes into contact with an infected individual from the current cell (i, j) or from eight neighbouring cells where ΣI_c and ΣI_a are the total infected individuals in the corners and adjacent cells, respectively.

(which is appropriate for dispersal in mammals; Poethke & Hovestadt, 2002) by the following function

$$D_{i,j} = d \exp \left(\frac{-(K_{i,j} - (S_{i,j} + I_{i,j}))}{0.5K_{i,j}} \right) \quad (3)$$

where d is the dispersal coefficient when the cell population is at its carrying capacity. There is no available data on the frequency of long-distance dispersals; therefore, we make an assumption that a squirrel will make approximately one long-range dispersal in its lifetime (when the density is at carrying capacity), thus giving $d = b$ (note that we do carry out sensitivity to this parameter in Section S6 in the Supplementary Information). Once an individual disperses from the focal cell, it enters one of the eight neighbouring cells at random depending on their cell density (with appropriate scaling between adjacent and corner cells).

Using methods of Gillespie (1977) (see also Keeling & Rohani, 2008 and Renshaw, 1993), we transform the rates into probabilities by dividing each rate by the sum of the total rates $R = \Sigma$ [*rates*] (see Table 1). The choice of event is determined at random and the time between events is defined as $\delta t = -(\ln(\psi))/R$ where ψ is drawn from a uniform distribution between 0 and 1 (which assumes that time to the next event is an exponentially distributed random variable; Renshaw, 1993). After each event grid cell densities and therefore probabilities are updated. By repeating this process, the abundance of susceptible and infected individuals in each cell can be tracked over space and time. A more detailed description of the model process is given in Section S1 of the Supplementary Information.

Arran connectivity

GIS data provide habitat information that is transformed into grid cell carrying capacity and informs within-cell epidemiological dynamics and between-cell transmission and dispersal. In addition to the GIS data, ground-truthing in collaboration with FCS has identified further routes of poor connectivity, highlighting, for instance, exposed mountain

tops that would be a barrier to dispersal. This can be incorporated in the model by preventing dispersal between appropriate cells (shown by black lines in Fig. 1b). The ground-truthing information is likely to impact dispersal and disease spread predicted by our model because, for example, in the middle of the island a barrier in Fig. 1b prevents east to west connectivity. In this study, we compare two connectivity scenarios: the first includes all the connectivity information obtained from GIS and ground-truthing, whereas the second uses GIS data only. It is likely that the connectivity in most spatial models utilizes GIS information only, so in comparing the two scenarios we aim to highlight the importance of incorporating local knowledge (if available) when modelling disease spread.

Parameter values

All demographic parameters are kept constant. The natural death rate, $b = 0.9$ yr^{-1}, is produced using adult mortality estimates presented in Barkalow, Hamilton & Soots (1970). The growth rate for red squirrels is estimated at 0.6 yr^{-1} (Tompkins *et al.*, 2003), which translates into a birth rate $a = 1.5$ yr^{-1}. The values of a and b combine with grid cell dependant carrying capacities to determine the susceptibility to crowding q in each patch. As detailed in The Model section dispersal rate $d = b$ and core movement has a range of $\alpha = 0.3$ km (Bosch & Lurz, 2012).

Table 2 displays the four sets of parameter values used for evaluating disease spread on Arran (note that the non-disease-related parameters remain fixed). In the absence of detailed information on red–red squirrel transmission rates of SQPV, previous modelling studies have simulated a range of potential values (e.g. Rushton *et al.*, 2000, 2006 where encounter rates were density dependent and values for the likelihood of infection for individuals were chosen by sampling deviates from a uniform range of 0–1); or have chosen grey–grey transmission values derived from antibody blood sampling data (Sainsbury *et al.*, 2000) as a benchmark value (e.g. Tompkins *et al.*, 2003; White *et al.*, 2014) and in each case undertook sensitivity analyses to assess the impacts of

Table 2 The disease parameters (in years^{-1} unless otherwise stated) considered in this study

Parameter	Acute (high virulence)		Chronic (low virulence)	
	Low transmission	High transmission	Low transmission	High transmission
Natural birth rate, a	1.5	1.5	1.5	1.5
Natural death rate, b	0.9	0.9	0.9	0.9
Core movement range, α (in km)	0.3	0.3	0.3	0.3
Dispersal rate, d	0.9*	0.9*	0.9	0.9
Transmission coefficient, β (km^2 y^{-1})	0.6	12	0.6	12
Disease induced death, σ	26	26	0.445	0.445

The models sensitivity to dispersal rate d has been tested in Section S6 of the Supplementary Information for the parameter sets denoted by *.

assumption. Here we follow the latter approach and use grey–grey squirrel transmission (acute, low transmission in Table 2) values as a lower benchmark and explore the implications of higher transmission scenarios. Because of the uncertainty of red–red transmission rates, we also consider an acute disease with high transmission (Table 2).

The variability in the disease spread has been linked to disease characteristics (Hess, 1996; Cross *et al.*, 2005). For example, Cross *et al.* (2005) found that a slow, chronic infection generally resulted in an increased number of infecteds when compared with a fast, acute infection. To provide a general understanding of disease spread on our complex landscape, we therefore consider disease parameters that represent chronic infections (low virulence) with low and high transmissibility (Table 2). Here virulence is chosen to maintain the same basic reproductive rate of the disease for the acute, high transmission and chronic, low transmission cases. Establishing these parameter sets allows us to examine the impact of different infectious disease characteristics on the spread and persistence of infection in fragmented habitats. (For further details on parameter estimation, see Section S3 of the Supplementary Information.)

Results

Squirrelpox spread on Arran

Assuming that SQPV transmission between red squirrels is the same as SQPV transmission between grey squirrels (acute, low transmission in Table 2), the spread of SQPV from its source of introduction is limited (Fig. 2). This indicates that there may be no large-scale threat to the population of red squirrels on Arran if an SQPV outbreak occurred. In most simulations, the disease fails to spread and fades out within 2 months of the initial introduction (Fig. 2a). In a few simulations (4 out of 25), there is limited disease spread to neighbouring cells but nevertheless the disease fades out within 6 months of the initial introduction (Fig. 2c). In all cases, the population reduction due to the disease is relatively small (infection within a grid cell reduces the density by at most 25%). Therefore, assuming the grey–grey parameter set for SQPV does not permit the spread of

disease or cause any significant reduction to the red squirrel population on Arran. This is due to the high virulence and low transmissibility of the disease which in combination with the relatively low densities on Arran (around 0.1–0.5 squirrels ha^{-1} around Brodick) means the basic reproductive rate of the disease (R_0) is not sufficiently high to promote large-scale disease spread or persistence (see Supplementary Information for a spatial analysis of R_0). Because disease spread is limited with these parameter values, there is no difference between the scenarios using GIS and ground-truthing and GIS information only.

Acute infection with high transmissibility

Figure 3 shows the population dynamics and disease spread when the high virulence of SQPV is retained and transmission is increased (acute, high transmission parameters in Table 2). When restrictions to dispersal imposed by ground-truthing are included, the disease spreads rapidly throughout the east and south of the island (region 1 in Fig. 1b). Disease outbreaks lead to a substantial reduction of up to 89% of local density. The density in region 1 is reduced to 15%, and the total population is reduced to 42% of its pre-infection levels. The wavelike expansion in the distribution of the disease and the eventual containment of disease is dependent on areas of high and low landscape connectivity. In areas of high connectivity, the disease spreads quickly causing high mortality; however, upon reaching regions of low connectivity the disease may fade out as it rapidly exhausts the local pool of susceptible individuals and is rarely able to spread over poor quality (low density) habitat (this prevents the spread from region 1 to 2 as denoted in Fig. 1b). When the additional barriers to dispersal imposed by ground-truthing are removed, the disease spread is more extensive and occurs across the majority of the island (as the connectivity between regions 1 and 2 is improved). There is high disease mortality in regions 1 and 2, and the total population is reduced to 22% of its pre-infection levels. Poor connectivity between regions 2 and 3 prevents disease outbreaks in region 3. In both connectivity scenarios, the disease fades out following an epidemic. Locally, this takes 1–2 months and typically fades out on the entire island within 7 months. Disease fade out arises from the rapid
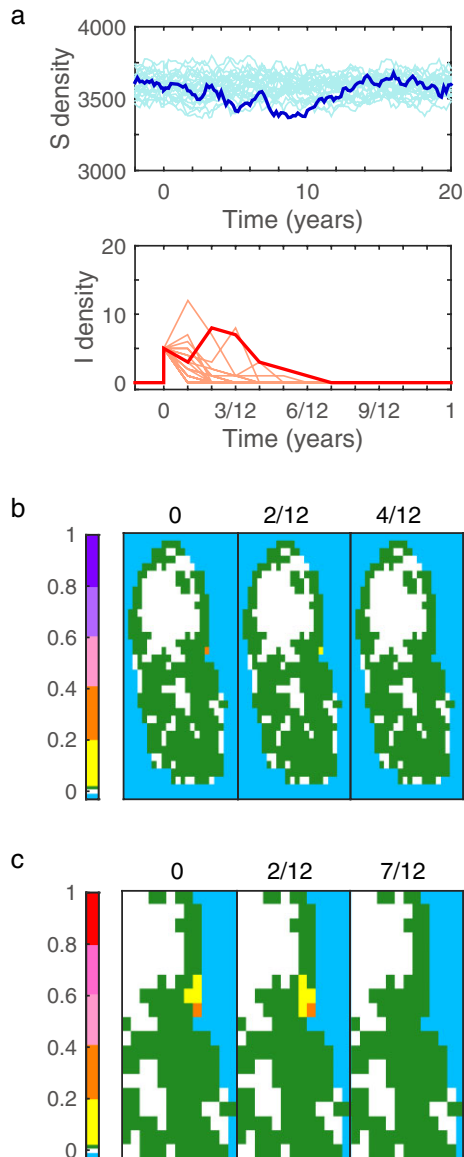
Figure 2 The model using grey–grey squirrelpox virus parameters (acute, low transmission in Table 2) where connectivity includes geographical information software information and ground-truthing. Once the total population has achieved quasi-steady state, five infected red squirrels are introduced at Brodick (Fig. 1a) at time 0. In (a) the total susceptible (blue) and infected (red) population densities are shown against time for 25 model realizations with a single realization highlighted. In (b) and (c), snap shots show the spatial distribution of disease at different time frames (identified, in years, in the title of each frame). We define the disease prevalence as the proportion of infected hosts in each cell [$Prev = (I_{i,j})/(I_{i,j} + S_{i,j})$]. In (b) we show the proportion of simulations that have a prevalence greater than 0.2. In (c) we show the prevalence for the realization highlighted in (a) with an enlarged scale to focus on the region where the disease was introduced.

spread of the highly virulent disease, which, largely exhausts the local population of susceptibles. Following the disease fade out, the population recovers to its pre-infection level through demographic processes. These simulations indicate that a highly virulent, highly transmissible disease can have marked impacts on the population density over a large scale. They also reveal how areas of low connectivity, through which the disease fails to spread, can protect populations from disease.

Chronic infection with low transmissibility

Figure 4 shows the impact of a chronic infection with low transmission (Table 2) when connectivity includes the information from ground-truthing (note, the basic reproductive rate of the disease, R_0, is the same in Figs 3 and 4, see Supplementary Information for further details). The disease initially spreads throughout region 1 reducing the population here to 17% of pre-infection levels, with the total population reduced to 43%. This outcome is similar to the acute, high transmission scenario with connectivity from GIS and ground-truthing (Fig. 3a–c) except for the chronic disease the rate of spread is reduced. The key difference is that the disease persists under this chronic scenario in the long term; therefore, a rare dispersal event eventually allows the disease to expand into region 2 in 80% and region 3 in 67% of realizations. Although the disease persists in the long term in a single realization of the model, the distribution of infection changes over time with periodic epidemics disease and fade out locally (Fig. 4c). (Results observed in the connectivity scenario in which the dispersal barriers imposed through ground-truthing are removed show a similar reduction to the host densities, but here the disease initially spreads to all regions.) A key difference between Figs 3 and 4 is that the persistence of chronic infection provides greater opportunity for dispersal and therefore it can eventually expand over a more extensive region.

For the remaining scenario, a chronic infection and high transmission in Table 2, the reproductive rate of the disease is greatly increased. Here, the disease spreads rapidly across the whole landscape, the total population abundance is reduced dramatically and most individuals become infected. This leads to the local extinction of populations. In the long term, there are two possible outcomes. Either the entire population becomes extinct or the disease becomes extinct and the population recovers to pre-infection levels (for more information see Section S5.3 in the Supplementary Information).

Results for all the scenarios presented here but with the low red squirrel density estimates used to determine grid cell carrying capacities are reported in Section S5 of the Supplementary Information. The results for the low-density scenarios are qualitatively similar to those for the high-density scenarios, although the effect of the lower density does reduce the severity of disease outbreaks and extent of disease spread (as at lower density the reproductive ratio of the disease, R_0, is reduced).
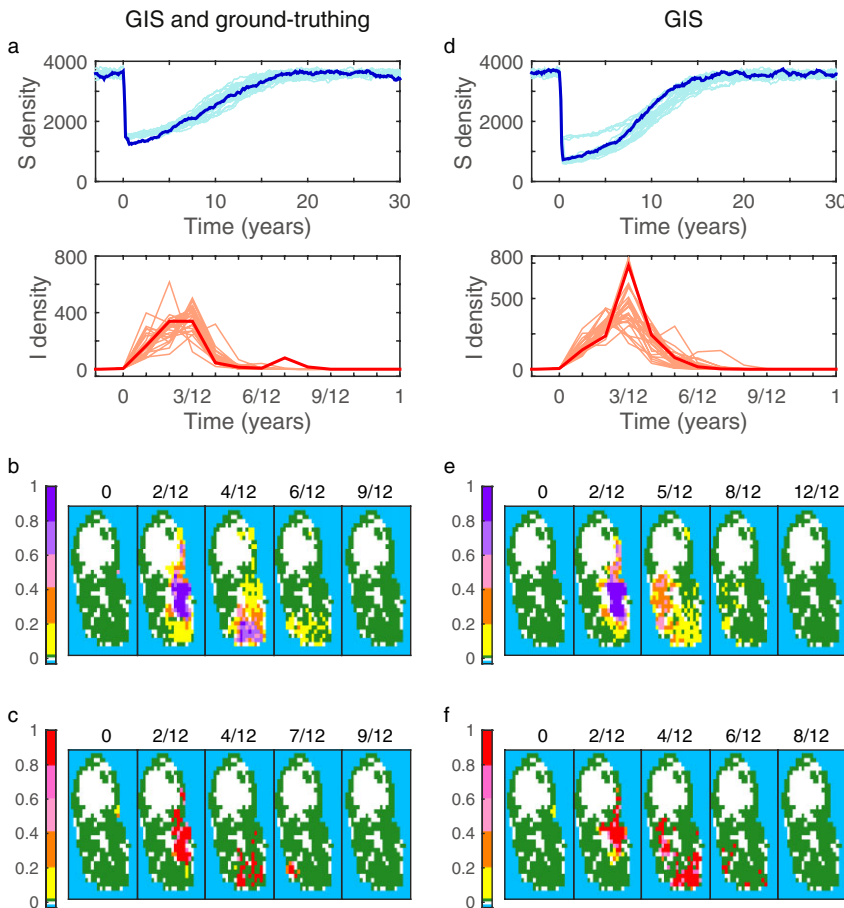
Figure 3 The model with acute, high transmission parameters (Table 2) where in (a)–(c) connectivity includes geographical information software (GIS) information and ground-truthing and in (d)–(f) GIS information only. Five infected red squirrels are introduced at Brodick (Fig. 1a) at time 0. In (a) and (d), the total susceptible (blue) and infected (red) population densities are shown against time for 25 model realizations with a single realization highlighted. In (b), (c), (e) and (f), snap shots show the spatial distribution of disease at different time frames (identified, in years, in the title of each frame). (b) and (e) show the proportion of simulations that have a prevalence greater than 0.2. (c) and (f) show the prevalence for the realization highlighted in (a) and (c), respectively. Further description is given in Fig. 2 caption.

We noted in The Model section that there is a lack of available data for determining the frequency of long-distance dispersals; thus, we set $d = b$ (Table 2) which assumes that on average a squirrel is likely to make one long-range dispersal in its lifetime. In Section S6 of the Supplementary Information, we carry out sensitivity analysis of parameter d for acute, low transmission and acute, high transmission parameter sets. We show that for both increase and decrease of the dispersal coefficient, the disease pattern is qualitatively similar to the results shown for the baseline parameter set. The lack of sensitivity to the dispersal parameter suggests that disease transmission may be driven by local spread within populations rather than the long-distance movement of infected individuals.

Discussion

EIDs and disease-mediated invasions are a substantial threat to native wildlife abundance and diversity (Morse, 1995; Daszak, 2000; Daszak *et al.*, 2001). Through the use of mathematical models, we addressed how infectious disease characteristics and landscape connectivity combined to influence disease spread and persistence. The model analysis allowed us to make system-specific predictions on the potential threat of SQPV to red squirrels on the Isle of Arran that are being used to influence conservation management decisions (Macpherson *et al.*, 2013). Further, the generality of our model framework allowed us to uncover broadly applicable findings on how different infection characteristics (acute or chronic infections) influence the spread and persistence of disease in realistic landscapes.

To protect the remaining populations of red squirrels, 35 red squirrel strongholds in England and Scotland have been developed in which reds are isolated from grey squirrels (through control of greys or due to the isolated nature of the stronghold). However, SQPV remains a threat to stronghold red populations. For instance, high-density red populations in Formby, Merseyside, and in Whinfell, Cumbria, have been protected by trapping and removal of greys as the launch of strongholds in 2006 (Parrott *et al.*, 2009; Chantrey *et al.*, 2014), but have suffered repeated SQPV outbreaks that has resulted in a marked reduction in population abundance (followed by the disease fading out and subsequent population increases). We argue that the simulated results using the landscape of Arran, despite being an island, are also representative of the mainland strongholds. A buffer area of trapping around the mainland strongholds removes greys; thus, it is unlikely that there will be more than one challenge at a time (although several may occur over a period of time) making our simulations a reasonable repre-
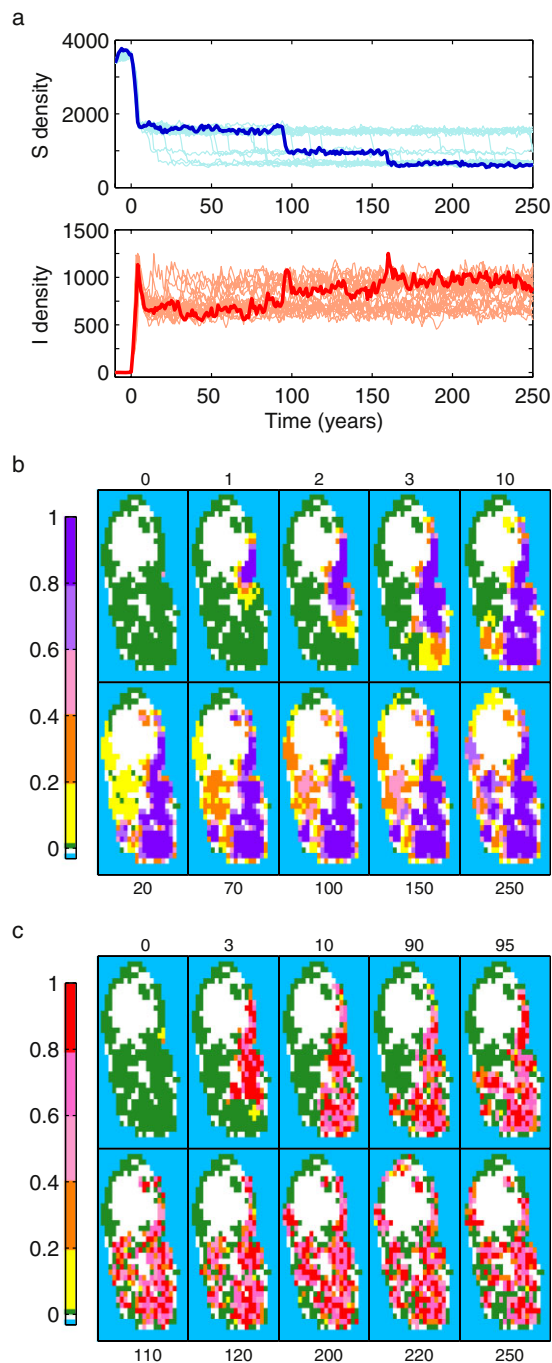
Figure 4 The model with chronic, low transmission parameters (Table 2) where connectivity includes geographical information software information and ground-truthing. Five infected red squirrels are introduced at Brodick (Fig. 1a) at time 0. In (a) the total susceptible (blue) and infected (red) population densities are shown against time for 25 model realizations with a single realization highlighted. In (b) and (c) snap shots show the spatial distribution of disease at different time frames (identified, in years, in the title of each frame) with (b) showing the proportion of simulations that have a prevalence greater than 0.2 and (c) showing the prevalence for the realization highlighted in (a). Further description is given in Fig. 2 caption.

sentation. Using grey–grey SQPV parameters, the model predicts the impact of disease on the low-density populations on Arran will be limited to a short-term, local outbreak focused at the point of disease introduction. When considering a highly virulent, highly transmissible disease (which could represent SQPV if red–red transmission is sufficiently higher than the grey–grey level or could represent a system where grey–grey transmission is accurate for SQPV in red squirrels and the population density is higher), the disease spread is more widespread and a substantial reduction in population density is predicted due to disease-induced mortality. However, disease spread does not occur between poorly connected regions and the disease fades out leading to population recovery to pre-infection levels, supporting the observations of disease dynamics in high-density stronghold populations (Parrott *et al.*, 2009). In terms of the conservation of red squirrels on Arran, the model suggests that if introduced, SQPV spread (using grey–grey transmission parameters) is likely to remain local to the point of introduction and will not cause an island-wide epidemic and as long as grey squirrels are removed from the island reds should recover.

The model results have broad implications for red squirrel conservation and more generally in the understanding of the spread of highly virulent EIDs through native populations. Our results support the previous studies of Duff, Holmes & Barlow (2010) and Gurnell *et al.* (2006) who concluded that in the absence of grey squirrels SQPV would not persist due to the increased mortality of reds reducing the chance of disease transmission. This suggests that the disease cannot persist without an additional local reservoir of infection and emphasizes that limiting grey squirrel introductions and/or preventing the further population expansion of grey squirrels may be critical to safeguarding the remaining red squirrel populations in the United Kingdom. The interface between the distribution of red and grey squirrels in the United Kingdom occurs in Highland Scotland and has been relatively stable for 40 years. Grey populations to the south of this interface are currently disease free, but recent surveys (Scottish Wildlife Trust, 2013) indicate that SQPV is spreading northwards from Southern Scotland and so there is a clear risk that SQPV will spread to grey populations at the interface. The model results here suggest the SQPV may cause epidemic outbreaks and mortality in red populations adjacent to the interface, but that it is unlikely to spread extensively through the red (only) populations in Highland Scotland (north of the interface). However, the impact of the disease will increase the apparent competition from greys at the interface (Tompkins *et al.*, 2003) and could allow greys to expand their distribution northwards (Bell *et al.*, 2008). This would have detrimental implications for the conservation of red squirrels and it is therefore essential that it is a focus for further study.

The implication of landscape connectivity for wildlife viability and persistence is well studied with clear evidence that increased connectivity can increase population abundance and prevent extinction (Fahrig & Merriam, 1985; Henein & Merriam, 1990; Schumaker, 1996; Dobson *et al.*,

1999; Lookingbill *et al.*, 2010; van Andel & Aronson, 2012). However, it has been argued that increased connectivity may also promote the spread of infectious disease (Hess, 1994; Bienen, 2002; Real & Biek, 2007). Previous theoretical studies have used idealized spatial set-ups to examine the impact of introduced infectious disease in fragmented landscapes. These studies have synthesized techniques from mathematical epidemiology with meta-population models (Hess, 1996; McCallum & Dobson, 2002) or developed stochastic simulation models based on underlying epidemiological frameworks that represent the dynamics on an array of patches connected in a simplified manner (Hess, 1996; White *et al.*, 2014). The most similar study to ours used an individual-based, stochastic disease model to represent the dynamics on a two-dimensional lattice of identical patches with nearest neighbour dispersal (Cross *et al.*, 2005). Findings indicate that improved connectivity can enhance the spread and persistence of disease, although the benefits of improved connectivity for population persistence may outweigh the disease risks (McCallum & Dobson, 2002). Also, local population interactions combine with infectious disease characteristic such that acute, highly virulent infection may fade out in a population whereas chronic, low virulence infection may be supported (Hess, 1996; Cross *et al.*, 2005).

Our study, which uses a realistic, heterogeneous, landscape based on habitat data, supports these findings. When the basic reproductive rate of the disease, R_0, is low (due to a combination of a low-density habitat, high virulence and low transmission), the disease fails to persist and spread is limited. When R_0 is increased, disease spread is more marked and the long-term impact depends on the nature, acute or chronic, of the disease. In particular, acute, highly transmissible infections can spread rapidly through regions of good habitat, but may fail to spread between poorly connected regions. The associated high virulence leads to severe population crashes and the disease therefore burns-out allowing populations to recover to pre-infection levels. Chronic infections spread more slowly, but can persist in regions of good habitat. This disease persistence provides increased opportunities for the disease to spread between poorly connected regions, and therefore chronic infections are more widespread. Using a realistic landscape, we have therefore been able to understand how high and low connectivity and fragmentation interact.

Evidence for different acute and chronic infection outbreaks has been identified in real-life systems. For example, epidemic outbreaks followed by the disease fading out has been observed in the high-density red squirrel population in the stronghold at Formby, Merseyside (Parrott *et al.*, 2009; Chantrey *et al.*, 2014). Alternatively, the squirrel Adenovirus may have similarities with the results of the chronic infection as it is less virulent than SQPV but can cause mortality when associated with other stress factors. Adenovirus has been reported in natural red squirrel populations that are free from grey squirrels with the disease persisting for many years (Martínez-Jiménez *et al.*, 2011; Everest *et al.*, 2013). Detailed investigations into the prevalence of

Adenovirus in red populations are ongoing (Everest *et al.*, 2013), but our modelling results suggest that the chronic nature of the disease may allow it to spread and persist should it be introduced into a naive population, such as the red population on Arran.

The results of our study highlight how wildlife management strategies should carefully consider the risk of disease outbreaks. Management strategies that increase population connectivity or increase population density (e.g. through supplementary feeding or changes to forest composition) may increase the risk of disease spread and so scale and location of such measures should be considered carefully. Our study has shown how stochastic modelling frameworks incorporating realistic habitat data are essential tools for the evaluation of such management strategies, and have wide application in the development of conservation planning, for both population stability and disease resilience.

References

van Andel, J. & Aronson, J. (2012). *Restoration ecology: the new frontier*. Chichester: John Wiley & Sons.

Barkalow, F., Hamilton, R. & Soots, R. Jr. (1970). The vital statistics of an unexploited gray squirrel population. *J. Wildl. Mgmt.* **34**, 489–500.

Beier, P. & Noss, R. (1998). Do habitat corridors provide connectivity? *Conserv. Biol.* **12**, 1241–1252.

Bell, S.S., White, A., Sherratt, J.A. & Boots, M. (2008). Invading with biological weapons: the role of shared disease in ecological invasion. *Theor. Ecol.* **2**, 53–66.

Bienen, L. (2002). Informed decisions conservation corridors and the spread of infectious disease. *Conserv. Pract.* **3**, 10–17.

Bosch, S. & Lurz, P.W.W. (2012). The Eurasian red squirrel. *Westarp Wissenschaften*.

Chantrey, J., Dale, T., Read, J., White, S., Whitfield, F., Jones, D., McInnes, C. & Begon, M. (2014). European red squirrels population dynamics driven by squirrelpox at a gray squirrel invasion interface. *Ecol. Evol.* **4**, 3788–3799.

Chesser, R. & Ryman, N. (1986). Inbreeding as a strategy in subdivided populations. *Evolution* **40**, 616–624.

Cross, P.C., Lloyd-Smith, J.O., Johnson, P.L. & Getz, W.M. (2005). Duelling timescales of host movement and disease recovery determine invasion of disease in structured populations. *Ecol. Lett.* **8**, 587–595.

Daszak, P. (2000). Emerging infectious diseases of wildlife – threats to biodiversity and human health. *Science* **287**, 443–449.

Daszak, P., Cunningham, A.A. & Hyatt, A.D. (2001). Anthropogenic environmental change and the emergence of infectious diseases in wildlife. *Acta Trop.* **78**, 103–116.

Dobson, A., Ralls, K., Foster, M., Soule, M.E., Simberloff, D., Doak, D., Estes, J.A., Mills, L.S., Mattson, D., Dirzo, R., Arita, H., Ryan, S., Norse, E.A., Noss, R.F. & Johns, D. (1999). 'Connectivity: maintaining flows in

fragmented landscapes'. In *Continental conservation: scientific foundations of regional reserve networks*, 129–170. Soule, M.E. & Terborgh, J. (Eds). Washington, DC: Island Press.

Duff, J., Holmes, J. & Barlow, A. (2010). Surveillance turns to wildlife. *Vet. Rec.* **167**, 154–156.

Everest, D.J., Butler, H., Blackett, T., Simpson, V.R. & Shuttleworth, C.M. (2013). Adenovirus infection in red squirrels in areas free from grey squirrels. *Vet. Rec.* **173**, 199–200.

Fahrig, L. & Merriam, G. (1985). Habitat patch connectivity and population survival. *Ecology* **66**, 1762–1768.

Gillespie, D. (1977). Exact stochastic simulation of coupled chemical reactions. *J. Phys. Chem.* **81**, 2340–2361.

Gurnell, J., Rushton, S., Lurz, P., Sainsbury, A.W., Nettleton, P., Shirley, M., Bruemmer, C. & Geddes, N. (2006). Squirrel poxvirus: landscape scale strategies for managing disease threat. *Biol. Conserv.* **131**, 287–295.

Hanski, I. (1998). Metapopulation dynamics. *Nature* **396**, 41–49.

Hanski, I. & Gilpin, M. (1991). Metapopulation dynamics: brief history and conceptual domain. *Biol. J. Linn. Soc.* **42**, 3–16.

Henein, K. & Merriam, G. (1990). The elements of connectivity where corridor quality is variable. *Landsc. Ecol.* **4**, 157–170.

Hess, G. (1994). Conservation corridors and contagious disease: a cautionary note. *Conserv. Biol.* **8**, 256–262.

Hess, G. (1996). Disease in metapopulation models: implications for conservation. *Ecology* **77**, 1617–1632.

Joint Nature Conservation Committee (2012). *UK biodiversity action plan*.

Kareiva, P. & Wennergren, U. (1995). Connecting landscape patterns to ecosystem and population processes. *Nature* **373**, 299–302.

Keeling, M.J. (1999). The effects of local spatial structure on epidemiological invasions. *Proc. Biol. Sci.* **266**, 859–867.

Keeling, M.J. & Rohani, P. (2008). *Modeling infectious diseases in humans and animals*. Princeton: Princeton University Press.

Levins, R. (1969). Some demographic and genetic consequences of environmental heterogeneity for biological control. *Bull. Entomol. Soc. Am.* **15**, 237–240.

Lookingbill, T.R., Gardner, R.H., Ferrari, J.R. & Keller, C.E. (2010). Combining a dispersal model with network theory to assess habitat connectivity. *Ecol. Appl.* **20**, 427–441.

Lurz, P., Geddes, N. & Lloyd, A. (2003). Planning a red squirrel conservation area: using a spatially explicit population dynamics model to predict the impact of felling and forest design plans. *Forestry* **76**, 93–106.

Lurz, P.W.W. (1995). *Ecology and conservation of the red squirrel (Sciurus vulgaris L.) in upland conifer plantations*. PhD thesis, University of Newcastle.

Lurz, P.W.W. (2012). *Arran red squirrel assessment*. Unpublished Technical Report.

Macpherson, M., Davidson, R., Duncan, D., White, A., Lurz, P. & Jarrett, A. (2013). *Assessing the impact of the squirelpox virus on Eurasian Red squirrel*. Unpublished Technical Report.

Manchester, S. & Bullock, J. (2000). The impacts of non-native species on UK biodiversity and the effectiveness of control. *J. Appl. Ecol.* **37**, 845–864.

Martínez-Jiménez, D., Graham, D., Couper, D., Benkö, M., Schöniger, S., Gurnell, J. & Sainsbury, A.W. (2011). Epizootiology and pathologic findings associated with a newly described adenovirus in the red squirrel, *Sciurus vulgaris*. *J. Wildl. Dis.* **47**, 442–454.

McCallum, H. & Dobson, A. (2002). Disease, habitat fragmentation and conservation. *Proc. Biol. Sci.* **269**, 2041–2049.

Morse, S.S. (1995). Factors in the emergence of infectious diseases. *Emerg. Infect. Dis.* **1**, 7–15.

Ostfeld, R.S., Glass, G.E. & Keesing, F. (2005). Spatial epidemiology: an emerging (or re-emerging) discipline. *Trends Ecol. Evol.* **20**, 328–336.

Parrott, D., Quy, R., Driel, K.V. & Lurz, P. (2009). *Review of red squirrel conservation activity in northern England*. Technical Report September, Natural England.

Patz, J.A., Daszak, P., Tabor, G.M., Aguirre, A.A., Pearl, M., Epstein, J., Wolfe, N.D., Kilpatrick, A.M., Foufopoulos, J., Molyneux, D., Bradley, D.J. & Emergence, D. (2004). Unhealthy landscapes: policy recommendations on land use change and infectious disease emergence. *Environ. Health Perspect.* **112**, 1092–1098.

Poethke, H.J. & Hovestadt, T. (2002). Evolution of density- and patch-size-dependent dispersal rates. *Proc. Biol. Sci.* **269**, 637–645.

Real, L.A. & Biek, R. (2007). Spatial dynamics and genetics of infectious diseases on heterogeneous landscapes. *J. R. Soc. Interface* **4**, 935–948.

Renshaw, E. (1993). *Modelling biological populations in space and time*, Vol. 11. Cambridge: Cambridge University Press.

Riley, S. (2007). Large-scale spatial-transmission models of infectious disease. *Science* **316**, 1298–1301.

Rushton, S., Lurz, P., Gurnell, J. & Fuller, R. (2000). Modelling the spatial dynamics of parapoxvirus disease in red and grey squirrels: a possible cause of the decline in the red squirrel in the UK? *J. Appl. Ecol.* **37**, 997–1012.

Rushton, S., Lurz, P., Gurnell, J., Nettleton, P., Bruemmer, C., Shirley, M. & Sainsbury, A. (2006). Disease threats posed by alien species: the role of a poxvirus in the decline of the native red squirrel in Britain. *Epidemiol. Infect.* **134**, 521–533.

Sainsbury, A.W., Nettleton, P., Gilray, J. & Gurnell, J. (2000). Grey squirrels have high seroprevalence to a

parapoxvirus associated with deaths in red squirrels. *Animal Conserv.* **3**, 229–233.

Schumaker, N. (1996). Using landscape indices to predict habitat connectivity. *Ecology* **77**, 1210–1225.

Scottish Wildlife Trust. (2013). *Annual report and financial statements for the year ended 31st March 2013*. Technical Report March.

Smith, K.F., Sax, D.F. & Lafferty, K.D. (2006). Evidence for the role of infectious disease in species extinction and endangerment. *Conserv. Biol.* **20**, 1349–1357.

Tompkins, D.M., Sainsbury, A.W., Nettleton, P., Buxton, D. & Gurnell, J. (2002). Parapoxvirus causes a deleterious disease in red squirrels associated with UK population declines. *Proc. Biol. Sci.* **269**, 529–533.

Tompkins, D.M., White, A.R. & Boots, M. (2003). Ecological replacement of native red squirrels by invasive greys driven by disease. *Ecol. Lett.* **6**, 189–196.

Tonkin, J.M. (1983). *Ecology of the red squirrel (Sciurus vulgaris) in mixed woodland*. PhD thesis, University of Bradford.

Travis, J.M.J. (2003). Climate change and habitat destruction: a deadly anthropogenic cocktail. *Proc. Biol. Sci.* **270**, 467–473.

Westervelt, J.D., Shapiro, M., Goran, W.D. & Gerdes, D.P. (1992). *Geographic Resources Analysis Support System (GRASS) version 4.0 user's reference manual*. US Army Corps of Engineers, Construction Engineering Research Laboratory.

White, A., Bell, S.S., Lurz, P.W. & Boots, M. (2014). Conservation management within strongholds in the face of disease-mediated invasions: red and grey squirrels as a case study. *J. Appl. Ecol.* **51**, 1631–1642.

Worrell, R. (2012). *An assessment of the potential impacts of ash dieback in Scotland*. Technical Report January, The Forestry Commission, Edinburgh.

Supporting information

Additional Supporting Information may be found in the online version of this article at the publisher's web-site:

Figure S1. The Isle of Arran is shown in (a) (with permission from FCS) with the coniferous (green) and broadleaf (brown) woodland highlighted and 'Br' represents the main port Brodick. The carrying capacity of red squirrels (per km^2) is shown in (b) which uses lower density estimates of abundance of 0:08 ha^{-1} in coniferous and 0:5 ha^{-1} in broadleaf representative of a poor seed year. Cells that are well connected are grouped together by the dashed olive blocks (labelled regions 1–3); there is poor connectivity between the blocks. In addition, ground-truthing in collaboration with Forestry Commission Scotland has identified routes that do not permit movement, identified by thick black lines.

Figure S2. A grid of nine cells (in blue) is shown in (a) with focal cell (i; j) highlighted in dark blue. A green buffer around the focal cell highlights the maximum red squirrel core range movement (with diameter α km) from neighbouring cells to the focal cell and vice versa. A horizontal cross-section across cells (i; $j - 1 : j + 1$) in (a) shows the possible density of (b) infected and (c) susceptible hosts. The area under these curves shows the total number of infected hosts interacting with the susceptible hosts from the focal cell.

Figure S3. The spatial, stochastic SI model in absence of disease for a (a–c) high seed year and a (d–f) low seed year. The total population densities are shown in grey against time for 25 model realizations with connectivity established from GIS information only in (a, d) and GIS information and ground-truthing in (b, e). The carrying capacity is shown in red. (c) and (f) show the cell densities on Arran at three time frames for the realization highlighted in (b) and (e), respectively. Parameters are given in Section S3.

Figure S4. The spatial, stochastic SI model with acute, high transmission parameters (Table 2) in a poor seed year where in (a)–(c) connectivity includes GIS information and ground-truthing and in (d)–(f) GIS information only. Five infected red squirrels are introduced at Brodick (Fig. S1a) at time 0. In (a) and (d) the total susceptible (blue) and infected (red) population densities are shown against time for 25 model realizations with a single realization highlighted. In (b), (c), (e) and (f), snap shots show the spatial distribution of disease at different time frames (identified, in years, in the title of each frame). (b) and (e) show the proportion of simulations that have a prevalence greater than 0:2. (c) and (f) show the prevalence for the realization highlighted in (a) and (c), respectively. Further description is in Fig. 2 caption.

Figure S5. The spatial, stochastic SI model with chronic, low transmission parameters (Table 2) in a poor seed year where in (a)–(d) connectivity includes GIS information and ground-truthing and in (e)–(h) GIS information only. Five infected red squirrels are introduced at Brodick (Fig. S1a) at time 0. In (a), (c), (e) and (h) the total susceptible (blue) and infected (red) population densities are shown against time for 25 model realizations with a single realization highlighted. (b), (d), (f) and (h) show the cell density maps for the realization highlighted in (a), (c), (e) and (h), respectively.

Figure S6. The spatial, stochastic SI model with chronic, high transmission parameters (Table 2) in a high seed year where in (a)–(d) connectivity includes GIS information and ground-truthing and in (e)–(h) GIS information only. Once the total population has achieved quasi-steady state, five infected red squirrels are introduced at Brodick (Fig. S1a) at time 0. In (a), (c), (e) and (g), the total susceptible (blue) and infected (red) population densities are shown against time for 25 model realizations with a single realization highlighted. In (b), (d), (f) and (h), the cell density maps are shown for the realizations highlighted in (a), (c), (e) and (g), respectively.

Figure S7. The spatial, stochastic SI model with acute, low transmission parameters (Table 2) in a high seed year where the dispersal coefficient is (a)–(b) $d = 0:5b$ and (c)–(d) $d = 2b$. The connectivity in all figures includes GIS information and ground-truthing. (a) and (c) show the total susceptible (blue) and infected (red) population densities against time for 25

model realizations. (b) and (d) show the proportion of simulations that have a prevalence greater than 0.2.

Figure S8. The spatial, stochastic SI model with acute, high transmission parameters (Table 2) in a high seed year where the dispersal coefficient is (a)–(b) $d = 0.5b$ and (c)–(d) $d = 2b$. The connectivity in all figures includes GIS information and ground-truthing. (a) and (c) show the total susceptible (blue) and infected (red) population densities against time for 25 model realizations. (b) and (d) show the proportion of simulations that have a prevalence greater than 0.2.

Table S1. The value of R_0 from equation (S4) is given in Table 2 in the main paper and the median carrying capacity $K = 9$ and $K = 4$ for high- and low-density estimates, respectively.

Section S1. Detailed model procedure.
Section S2. Red squirrel carrying capacity for a poor seed year.
Section S3. Parameterization of model.
Section S4. Model simulations in the absence of disease.
Section S5. Further results from the disease model.
Section S5.1. High transmission, acute disease in a poor seed year.
Section S5.2. Low transmission, chronic disease in a poor seed year.
Section S5.3. High transmissible, chronic disease.
Section S6. Sensitivity to dispersal parameter d.